EXPERIMENTAL IDENTIFICATION OF CP-Cu YIELD SURFACE AND ITS EVOLUTION DUE TO COMPLEX LOADING PRE-DEFORMATION

Ved Prakash DUBEY, Mateusz KOPEC*◉, Zbigniew L. KOWALEWSKI

Institute of Fundamental Technological Research, Polish Academy of Sciences, Warsaw, Poland
*corresponding author, *mkopec@ippt.pan.pl*

This study examines the yield surface evolution of technical copper (CP-Cu) under complex loading, focusing on monotonic tension and combined tension with cyclic torsion. Using biaxial testing, initial and pre-deformed yield surfaces were analysed. Results indicate kinematic hardening with tensile pre-strain, while cyclic torsion induces anisotropic hardening at lower amplitudes ($\pm 0.1\,\%$) and softening at higher amplitudes ($\pm 0.2\,\%$). Strain amplitude significantly impacts material response, while frequency has a minor effect.

Keywords: copper; pre-deformation; yield surface; biaxial.

1. Introduction

Copper, a versatile and highly conductive material, serves as a fundamental element in various engineering and industrial applications due to its exceptional mechanical, thermal, and electrical properties. Its alloys, such as bronze and brass, further expand its utility by enhancing characteristics such as strength, corrosion resistance, and wear resistance (Zhang *et al.*, 2024). Copper and its alloys are extensively used in sectors like electronics, electrical engineering, construction, automotive, and aerospace industries. The mechanical properties of copper, such as ductility, toughness, high thermal conductivity ($400\,\mathrm{W/m \cdot K}$), high electrical conductivity ($5.8 \times 10^7\,\mathrm{S/m}$), and low electrical resistivity ($1.72 \times 10^{-8}\,\Omega$), make it indispensable for manufacturing heat exchangers, electrical wires, printed circuit boards, and architectural elements (Vahedi Nemani *et al.*, 2024). However, understanding the mechanical behaviour of copper under different manufacturing conditions and loading situations is crucial for optimizing its performance and reliability in these applications. The mechanical properties of copper are closely related to its purity, microstructure, and the presence of alloying elements. Pure copper exhibits excellent ductility and thermal conductivity, with a tensile strength usually ranging between $200\,\mathrm{MPa}$ and $300\,\mathrm{MPa}$ and an elongation at break of up to $50\,\%$ in annealed conditions (Guschlbauer *et al.*, 2018; Li & Zinkle, 2012). Its yield strength is comparatively lower, approximately $70\,\mathrm{MPa}$ in a pure, annealed form, but can be significantly enhanced through alloying and work-hardening

Ministry of Science and Higher Education
Republic of Poland

(Guschlbauer *et al.*, 2018; Lai *et al.*, 2022). For example, copper-zinc alloys (brass) provide improved strength and machinability, with yield strengths reaching up to 600 MPa, while copper-tin alloys (bronze) are favoured for their corrosion resistance and higher tensile strength, reaching up to 700 MPa (Scudino *et al.*, 2015; Semih & Recep, 2023; Wu *et al.*, 2013).

Applications in the electrical industry demand high conductivity, which necessitates minimal alloying. In contrast, structural and mechanical applications prioritize strength and wear resistance, often achieved through alloying with elements like aluminium, titanium, silicon, or nickel (Czerwinski, 2024; Pingale *et al.*, 2021; Zhou *et al.*, 2023). The interplay of these properties underlines the need for a detailed understanding of the material's mechanical behaviour during various manufacturing processes.

Manufacturing techniques significantly influence the mechanical properties of copper and its alloys. Processes such as casting, forging, extrusion, rolling, and additive manufacturing introduce variations in grain size, texture, and residual stress, which affect yield strength and deformation behaviour (Jiang *et al.*, 2021; Zhang *et al.*, 2024). Several studies have investigated the impact of pre-deformation and manufacturing techniques on the mechanical properties of copper and its alloys. Pre-deformation, such as cold rolling or tension, modifies the microstructure of copper by inducing dislocations and work hardening. For example, Stepanov *et al.* (2012) demonstrated the effect of cold rolling on the microstructure and mechanical properties of copper processed via equal channel angular pressing (ECAP). It reveals that cold rolling transforms the equiaxed grains formed during ECAP into a lamellar structure. This process enhances yield strength by 100 MPa due to reduced boundary spacing, aligning with the Hall–Petch relationship. Additionally, dynamic restoration increases high-angle boundary fractions, reflecting microstructural refinement and strengthening. Sungar Singh Sivam *et al.* (2023) examined unidirectional rolling (UDR) and cross-rolling (CR) of pure copper, revealing distinct mechanical responses. UDR achieves higher tensile strength (324 MPa) and hardness (98.2 HV) compared to CR (310 MPa and 95.4 HV, respectively) at a true strain of 2.77. UDR induces elongated grains and higher stored energy (0.69 J/g), while CR forms equiaxed grains with reduced anisotropy and lower stored energy (0.54 J/g). These microstructural changes, driven by deformation modes, explain the variations in mechanical properties. Results of research conducted by Pan *et al.* (2023) revealed significant enhancement in mechanical properties of pure copper processed with low-angle dislocation boundaries (LADBs). Initial coarse-grained (CG) copper had a yield strength of 61 MPa, tensile strength of 231 MPa, and a fatigue endurance limit of 50 MPa (fatigue ratio 0.24). After LADBs introduction, dislocation-cell-structured (DC) copper exhibited a yield strength of 372 MPa, tensile strength of 374 MPa, and a fatigue endurance limit of 130 MPa (fatigue ratio 0.35). This improvement is attributed to nanoscale dislocation patterns, reducing surface roughening and enhancing cyclic loading resistance.

The study of yield strength and yield surface evolution in copper and its alloys has been an active area of research. The yield surface is a graphical representation of the stress states at which a material begins to deform plastically. The yield surface reflects anisotropy and hardening behaviour, providing insights into the material's deformation mechanisms under complex loading conditions. This analysis of copper enables the design of components that can withstand multiaxial stresses encountered in practical applications, such as piping systems, automotive heat exchangers, and structural elements in buildings. Mair and Pugh (1964) analysed thin-walled tubes of annealed copper pre-strained to the values of 1.3 %, 4.7 %, and 8.5 % in tension or 0.25 %, 1.5 %, and 3 % in torsion, respectively. The results demonstrated yield locus expansions and cross-effects in both cases, such that tensile pre-strain increased torsional yield stress and torsional pre-strain increased yield stress in tension, contrary to the expectations of isotropic hardening. The torsional pre-strain displayed a significant Bauschinger effect, with the magnitude increasing with the increase in the pre-strain level. Hecker (1971) investigated yield surface evolution in annealed OFHC copper subjected to biaxial stress. Specimens pre-strained via

axial tension and internal pressure showed significant yield surface distortions and directional anisotropy at small proof strain (5 µε) levels. The initial yield surface expanded and translated in the direction of pre-strain either in axial or circumferential pre-strain and, for biaxial pre-strains, distorted in the vicinity of the loading point. Larger proof strains (2000 µε) mitigated these effects, resulting in isotropic expansion. Dietrich and Kowalewski (1997) explored the impact of pre-deformation on the yield surface of 99.9 % pure copper subjected to pre-strains of 5 % and 15 % of tension creep at 523 K and monotonic tension at ambient temperature. The investigations revealed that initial yield surfaces align with the isotropic Huber–von Mises criterion, but even minor plastic deformation introduces anisotropy. Pre-strain causes a disproportionate increase in yield surface axes, with monotonic loading inducing greater shifts than creep due to elevated-temperature exposure. Additionally, the major-to-minor axis ratio of the yield surface decreases significantly with small plastic pre-strain and stabilizes for higher pre-deformation for both pre-strain cases. These findings emphasize the role of deformation mechanisms in altering yield surface geometry and material anisotropy. This can be attributed to stress-induced texture development and subgrain formation that extended creep life and yield strength, with secondary creep rates reduced significantly for pre-strained copper. Helling *et al.* (1986) analysed multi-axial yield loci in 70:30 brass under torsional pre-strains ranging from 2.4 % to 32 %. Severe distortions and strong directional memory effects were observed, with yield surface translations of up to 80 % in comparison to the initial yield locus. Microstructural findings showed pronounced twin boundary motion and strain-induced grain refinement, contributing to yield locus shifts. The study also investigated the effects of directionality on yield surface distortion, i.e., the orientation of the flattened region on the yield locus. The results indicate that yield surface distortion is largely independent of the pre-stress path but is significantly influenced by the pre-strain path, with the final pre-strain direction exerting a dominant effect. A recent research conducted by Liu *et al.* (2023) investigates the yielding behaviour of TU00 pure copper under strain rates ranging from 10^{-3} s to 10^3 s using a servo-hydraulic axial-torsional testing machine and a combined tension-torsion Hopkinson bar system for dynamic tension-torsion tests. Yield stress increased significantly with the strain rate, from 120 MPa to 190 MPa, highlighting the strain rate dependency. The modified Hill yield criterion, incorporating strain rate effects, provided the most accurate predictions of yield points, while emphasizing that strain rate hardening is anisotropic with notable differences in tensile and torsional responses. A universal strain rate hardening model integrating the Johnson–Cook constitutive framework effectively described the work hardening behaviour of copper under complex stress states, aligning well with experimental data and demonstrating the limitations of uniaxial tensile tests alone for describing the strain hardening behaviour of TU00 copper.

Although substantial progress has been made in understanding the mechanical behaviour and the yield surface evolution of copper and its alloys, still several gaps remain. The effects of complex pre-deformation and multiaxial stress loading on the yield surface evolution have not been fully studied. Therefore, the main aim of this paper is to determine experimentally the initial yield surface of CP-Cu alloy, followed by subsequent yield surfaces reflecting plastic pre-deformation. The pre-deformation was introduced by monotonic tension and combined monotonic tension – proportional cyclic torsion loadings. By advancing the understanding of the yield surface evolution, this research seeks to provide insights for optimizing the mechanical performance of copper in various engineering applications.

2. Materials and methods

The material used in this study was commercially pure copper (CP-Cu). The copper bars used in this study were obtained in the M1E-Z4 condition, which corresponds to the Cu-ETP (M1E; E-Cu58) state. The copper bars were machined into thin-walled tubular specimens with identical inner and outer surface finishes, using consistent turning parameters to ensure unifor-

mity. The specimen geometry is illustrated in Fig. 1. Mechanical testing was conducted utilizing an MTS 858 servo-electrohydraulic biaxial testing machine at room temperature ($23\,°C$). This system has a maximum axial force capacity of $\pm 25\,kN$ and a maximum torque of $\pm 100\,Nm$. Uniaxial tensile tests were initially performed to determine the basic mechanical properties, including the conventional yield strength. Based on the stress-strain response, the pre-deformation criterion was defined.
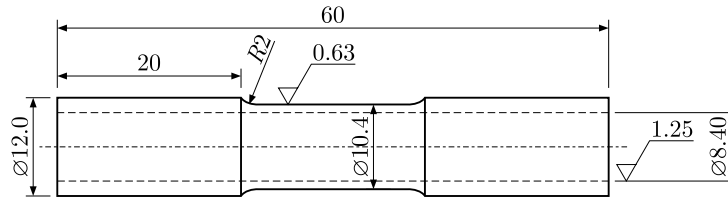

Fig. 1. Engineering drawing of the specimen.

Vishay $120\,\Omega$ strain gauges were affixed in the middle of the outer surface of the gauge section for the purpose of measuring and controlling strain components. Axial and shear strain components were recorded using a three-element $45°$ rectangular rosette (EA-05-125RA-120) with a $3.18\,mm$ gauge length, while hoop strain was measured using a linear pattern rosette (EA-13-062AK-120) with a $1.57\,mm$ gauge length. The strain gauges were bonded using M-Bond 610 adhesive, ensuring precise data acquisition. The three-element rosette configuration included a strain gauge aligned with the specimen's longitudinal axis for axial strain measurement, while the remaining two gauges, positioned at $+45°$ and $-45°$, formed a half-bridge circuit to measure shear strain. The hoop strain was measured using a separate half-bridge circuit perpendicular to the longitudinal axis (Dubey *et al.*, 2023). This setup, directly integrated with the testing machine controller, enabled accurate strain monitoring and control throughout the experiments.

To determine the initial and subsequent yield surfaces of CP-Cu, a single-specimen sequential probing technique was employed under strain-controlled loading. The loading sequence began with tension and returned to the same direction after completing all predefined stress paths. Each loading path started from the zero stress state and continued until a limited plastic offset strain of $0.02\,\%$ was reached, after which stress-controlled unloading was performed until the zero stress state. Yield points were determined using the specified offset strain method, defining yield as the point where the equivalent stress-strain curve deviated by $0.01\,\%$ from the elastic response in each loading direction (Kopec *et al.*, 2024). The numerical computation of the yield surface was conducted using the Szczepiński anisotropic yield criterion, and experimental yield points were fitted to the yield equation using the least squares method to ensure accuracy in characterizing the anisotropic mechanical behaviour of CP-Cu. The Szczepiński yield criterion extends the von Mises and Hill models by incorporating linear stress terms to account for deformation-induced anisotropy and the Bauschinger effect, capturing the directional dependence of the yield strength.

The experimental study of CP-Cu was carried out in three stages following a structured methodology. Firstly, the fundamental mechanical properties of CP-Cu were characterized. Thereafter, plastic pre-deformation was introduced in the specimens through two approaches: (a) monotonic tension loading up to $1\,\%$ of permanent strain, and (b) a combination of monotonic axial tension up to the same strain level with proportional cyclic torsional loading. The cyclic torsional loading was performed at two strain amplitudes ($\pm 0.1\,\%$ and $\pm 0.2\,\%$) and two frequencies ($0.5\,Hz$ and $1\,Hz$), as CP-Cu achieved a very limited value of axial stress ($15\,MPa$) at the $1\,\%$ axial pre-strain value at a higher strain amplitude equal to $\pm 0.4\,\%$, at a frequency of $0.5\,Hz$. Finally, the initial yield surface of the as-received CP-Cu was determined, along with the yield surfaces of the pre-deformed specimens.

3. Results and discussion

3.1. Mechanical properties of as-received material

Tensile tests were performed on solid tubular and thin-walled samples at room temperature at a constant strain rate of $0.005\,\mathrm{s}^{-1}$. Figure 2a shows the engineering stress-strain curve of CP-Cu, and its tensile properties are listed in Table 1. The minor variations in tensile results shown in Fig. 2a for both solid tubular and thin-walled specimens can be attributed to differences in specimen geometry, which may influence stress distribution and deformation characteristics. Comparing these findings with existing literature data is challenging, as the mechanical properties of commercially pure copper are highly sensitive to factors such as grain size, purity, processing, and heat treatment conditions. For reference, previous studies (Guschlbauer *et al.*, 2018; Jadhav *et al.*, 2021) report yield strengths ranging from $70\,\mathrm{MPa}$ to $300\,\mathrm{MPa}$ and tensile strengths between $150\,\mathrm{MPa}$ and $450\,\mathrm{MPa}$, depending on these variables. The yield and tensile strength values obtained in this study fall within these ranges, suggesting consistency with established trends while also emphasizing the inherent variability in mechanical properties due to processing conditions. Figure 2b presents the effective stress-strain curves comparing the material behaviour of thin-walled specimens subjected to tension, tension-torsion, and pure torsion. The stress-strain curves for torsion and tension-torsion loading closely overlap, whereas the curve for tension loading deviates significantly from the other two loadings, which indicates that the same material exhibits distinct mechanical responses under different loading conditions. These variations can likely be attributed to the initial anisotropy introduced during the manufacturing process, which affects how the material accommodates different stress states. This anisotropy influences the deformation mechanisms, leading to differences in stress distribution and strain accumulation under various loading paths.
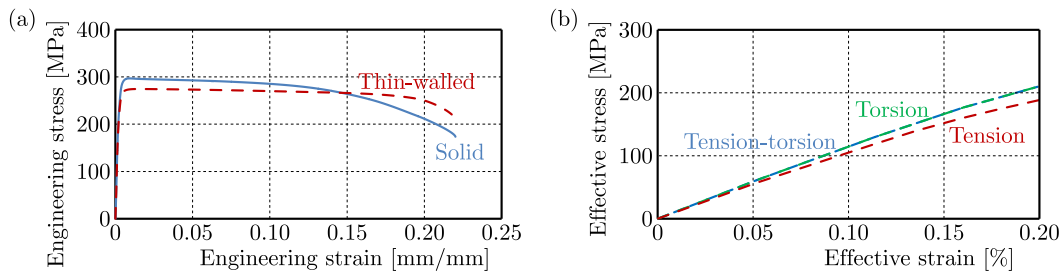

Fig. 2. (a) Tensile stress-strain response of solid and thin-walled CP-Cu specimens; (b) comparison of CP-Cu behaviour under various loading conditions.

Table 1. Mechanical properties of commercially pure copper.

	$R_{p0.2}$ [MPa]	R_m [MPa]	A [%]	E [GPa]
Solid specimen	286 (±2)	297 (±1)	22 (±1)	112 (±1)
Tubular specimen	264 (±2)	274 (±1)	21 (±1)	110 (±1)
ASTM standard (C11000) (Davis, 2001)	69–365	221–455	4–55	–

3.2. Mechanical response of CP-Cu under complex loading

The effect of the cyclic torsion with varying strain amplitudes and frequencies on the monotonic tensile behaviour of CP-Cu was investigated. The main aim was to induce plastic pre-deformation and examine changes in tensile characteristics under torsion-reverse-torsion cycling. Figures 3a and 3b demonstrate that the tensile characteristics of CP-Cu are significantly affected when tension is combined with cyclic torsion. A clear softening effect is observed, characterized by a decrease in axial stress as the cyclic strain amplitude increases. Additionally, an increase in
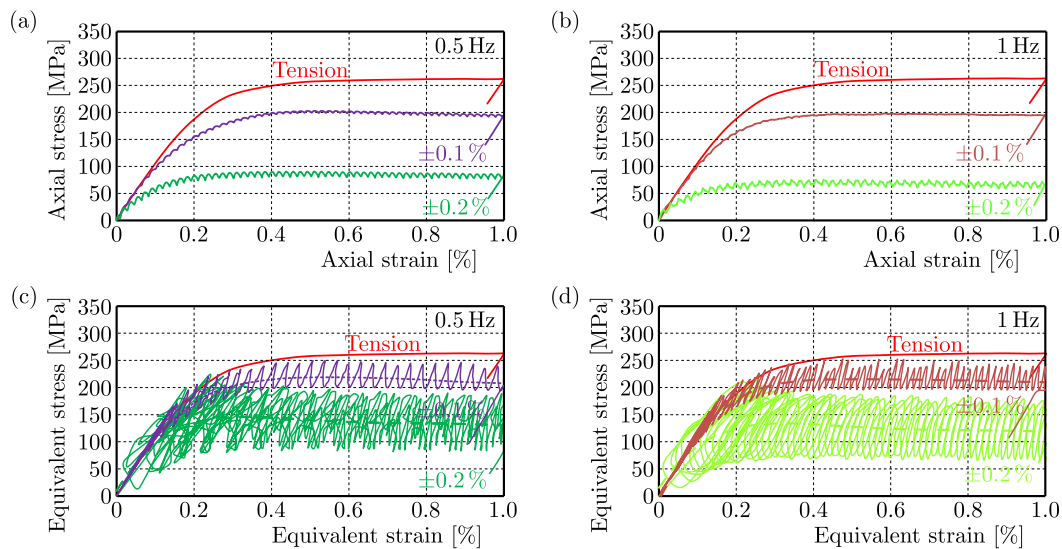
Fig. 3. Comparison of CP-Cu response in monotonic tension and tension with torsion-reverse-torsion at strain amplitudes of ±0.1 % and ±0.2 % for frequencies of 0.5 Hz (a, c) and 1 Hz (b, d).

cyclic torsion frequency further amplifies this decrease in the axial stress. For the cyclic torsion strain amplitude of ±0.1 % at the frequency of 0.5 Hz, the tensile stress at 0.2 % axial strain decreased from 188 MPa to 163 MPa. When the cyclic torsion strain amplitude increased to ±0.2 % at the same frequency, the decrease was more pronounced (80 MPa) at the same level of axial strain (Fig. 3a). The effect became even more significant at a higher frequency. For example, at ±0.2 % cyclic torsion strain amplitude and 1 Hz frequency, the tensile stress dropped from 188 MPa to 64 MPa, representing a 66 % reduction compared to the tension-only condition at 0.2 % axial strain (Fig. 3b).

This decrease in tensile stress is consistent with the influence of shear stress introduced during cyclic torsion. To better understand the effect of shear stress and evaluate the equivalence of stress under the three loading scenarios, Figs. 3c and 3d present the equivalent stress-strain curves. These curves provide a comprehensive representation of the material's response under combined tension and torsion loading. The equivalent stress-strain curves clearly demonstrate a pronounced softening effect in CP-Cu as the cyclic torsional strain amplitude increases. This trend aligns with the reduction in axial stress observed in Figs. 3a and 3b, suggesting that shear stress significantly alters the material's behaviour. The progressive reduction in equivalent stress at higher strain amplitudes highlights the combined effects of axial and torsional deformation, where shear stress introduces additional dislocation motion, enhancing plastic flow and reducing the material's load-bearing capacity.

The observed trend of decreasing tensile stress with increasing cyclic torsion is further illustrated in Fig. 4 for 0.5 % axial strain, evaluated across different cyclic torsion strain amplitudes and frequencies. Notably, the case of 0 % cyclic torsion strain amplitude corresponds to monotonic tension, serving as a baseline (Fig. 4a). The results clearly demonstrate a significant reduction in the tensile stress with the increasing cyclic torsion strain amplitude. In contrast, the impact of the increasing cyclic torsion frequency on tensile stress is comparatively less pronounced during combined loading (Fig. 4b). This suggests that the amplitude of torsional strain plays a dominant role in altering the stress state of copper by introducing additional shear deformation and facilitating plastic flow, whereas the role of frequency is primarily to modulate the rate at which these effects accumulate. The softening effect was also observed in CP-Ti with the increase in cyclic torsion strain amplitude and frequency during combined tension-torsion loading. These results indicate that the combination of cyclic torsion and tension leads to significant material softening, likely due to the accumulation of dislocation interactions and the
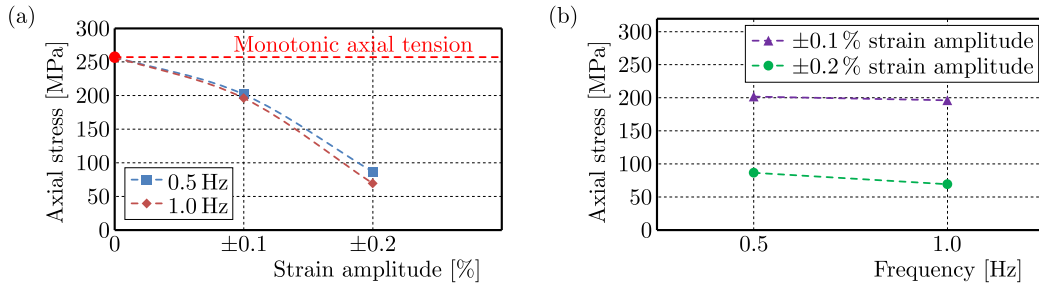
Fig. 4. Tensile stress variation at 0.5 % axial strain under combined tension-cyclic torsion for ±0.1 % and ±0.2 % (a) strain amplitudes and 0.5 Hz and 1 Hz (b) frequencies.

microstructural evolution under complex loading. The severity of the softening effect increases with both strain amplitude and frequency, emphasizing the need to account for such interactions when predicting the mechanical performance of CP-Cu in applications involving combined loading conditions.

3.3. Identification of the initial yield surface of CP-Cu

The yield surfaces of the CP-Cu in the as-received state were determined using a sequential loading procedure at offset strain values of 0.01 % and 0.005 %, as shown in Fig. 5a. These yield surfaces demonstrate a clear dependence on the chosen yield definition. After experimentally determining the yield points in various directions, ellipses were fitted using coefficients calculated via the least squares evaluation method. The primary parameters of these ellipses are summarized in Table 2, indicating that the centre of the yield surface is nearly aligned with the origin (0, 0) of the biaxial stress plane, with negligible rotation. Despite this alignment, some degree of initial anisotropy was evident, as the axis ratios of the yield surfaces were 1.34 and 1.37 – significantly lower than the isotropic value of 1.73 predicted by the Huber–von Mises yield criterion. This deviation highlights the anisotropic behaviour of the as-received material. While both yield definitions provided qualitatively similar yield surface shapes and anisotropic characteristics, the absolute values of the yield points and surface size differ, which emphasizes the need to carefully select the yield criterion based on the specific application. In applications requiring precise modelling of initial plastic yielding, a smaller offset may be more appropriate. However, for general engineering design, a larger offset is mostly selected.
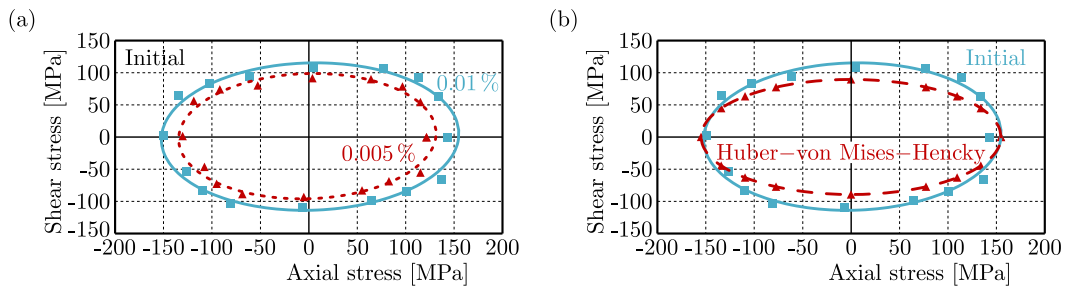

Fig. 5. Yield surfaces of as-received CP-Cu with yield points for 0.005 % (dotted red) and 0.01 % (continuous blue) offset strains (a); comparison of the initial yield surface with an isotropic yield surface (dashed red) (b).

Table 2. Ellipse parameters of the initial yield surfaces for CP-Cu.

	Centre (x_0, y_0) [MPa]	Rotation angle (Ø) [Radian]	Semi-axes (a, b) [MPa]	Axis ratio (a/b)
0.01 % offset strain	1.36, 0.60	0.07	153.78, 114.44	1.34
0.005 % offset strain	−1.45, 1.26	0.08	133.09, 97.17	1.37

To further investigate the material's initial anisotropy, the 0.01 % offset yield surface of CP-Cu was compared with an isotropic yield surface, anchored by the yield point in tension (direction 0). Figure 5b illustrates this comparison, showing that the axial yield stress of as-received CP-Cu aligns with the isotropic yield surface, while noticeable deviations occur in the shear stress direction. This discrepancy confirms the presence of initial anisotropy in the as-received material. The observed initial anisotropy is attributed to distinct hardening behaviour in shear strength, which likely results from the manufacturing processes applied to the material, such as the conversion of a solid specimen into a thin-walled tubular geometry or specific production methods used during material preparation. These processes induce microstructural variations, residual stresses, and texture development, which collectively contribute to the anisotropic response of CP-Cu.

3.4. Evolution of the CP-Cu yield surface due to pre-deformation

The effect of monotonic tension and a combination of monotonic tension with cyclic torsion pre-deformation on the mechanical properties of commercially pure copper was examined by studying changes in the initial yield surface. Pre-deformation tests were conducted until the specimens reached an axial strain of 1 %. Afterwards, the yield surfaces of the pre-deformed samples were determined using the same 0.01 % offset strain method as applied to the untreated specimen. Figure 6 presents the yield surface of CP-Cu following 1 % tensile pre-deformation in comparison to the initial yield surface. Although the overall shape remains consistent with the original yield surface, a distinct shift in the tensile direction is evident. This displacement suggests that monotonic tensile deformation has led to kinematic hardening along the direction of pre-strain. However, a decrease in the compressive direction and no change in the shear stress direction were observed. The increase in the tensile yield point is approximately 35 MPa, representing a 24 % enhancement over the initial yield point. This kinematic hardening effect can be attributed to the accumulation of dislocations and rearrangement of microstructural features during tensile pre-deformation, which results in an increase in material resistance to further plastic deformation in the pre-strain direction. The translation of the yield surface, rather than a uniform expansion, suggests that the material retains some degree of anisotropy following pre-deformation. This behaviour is consistent with the dislocation motion being predominantly oriented along the tensile direction, which reinforces the material's strength and shifts the yield surface correspondingly. The observed kinematic hardening in CP-Cu is crucial for metal forming processes, as pre-straining induces directional strengthening and it also influences fatigue performance in cyclic-loaded components by reducing reverse loading resistance.
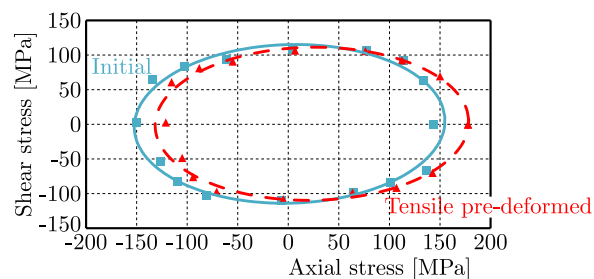

Fig. 6. Comparison of yield surfaces for pure copper: initial vs. after tensile pre-deformation.

Figure 7 illustrates the yield surfaces of CP-Cu following pre-deformation resulting from monotonic tension coupled with proportional torsion-reverse-torsion cyclic loading. These yield surfaces are evaluated against the initial yield surface of the material in its as-received condition (represented by a continuous line). The applied preloading leads to either anisotropic hardening or softening, influenced by the amplitude and frequency of the torsional strain during pre-deformation. For a torsional strain amplitude of ±0.1 % at a frequency of 0.5 Hz, the tensile
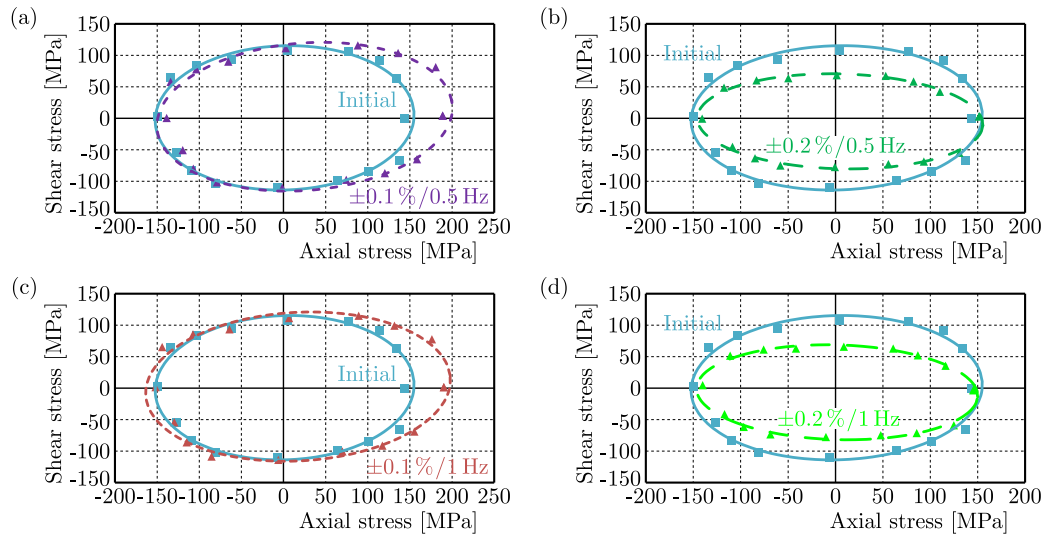
Fig. 7. Initial and pre-deformed yield surfaces of CP-Cu under combined tension and cyclic torsion ($\pm 0.1\,\%$ and $\pm 0.2\,\%$ strain amplitudes, $0.5\,\mathrm{Hz}$ and $1\,\mathrm{Hz}$ frequencies).

yield stress increases by approximately $46\,\mathrm{MPa}$ compared to the initial yield surface, while yield stresses in other directions remain largely unchanged (Fig. 7a). The observed anisotropic hardening is likely linked to a more uniform dislocation distribution and the formation of low-energy dislocation structures, such as subgrain formation, which enhance resistance to plastic deformation in particular directions. This resulted in an expansion of the initial yield surface in the tensile direction, reflecting an increased yield strength across tensile dominated stress paths. A similar trend is observed when the frequency is increased to $1\,\mathrm{Hz}$ (Fig. 7c), suggesting that the low-amplitude cyclic torsion predominantly reinforces the material in the axial stress direction. Conversely, for a torsional strain amplitude of $\pm 0.2\,\%$ at $0.5\,\mathrm{Hz}$, the yield surface exhibits a reduction in the shear stress direction by $32\,\mathrm{MPa}$–$38\,\mathrm{MPa}$, while axial stress values remain comparable to those of the initial yield surface (Fig. 7b). The observed anisotropic softening can be associated with shear band formation, dislocation glide along specific planes, and localized microstructural rearrangements due to large shear strains (Gazder *et al.*, 2006), which may reduce the material's resistance to shear loading. Increasing the frequency to $1\,\mathrm{Hz}$ produces similar results, with a decrease in shear stress and a negligible change in the axial stress (Fig. 7d). This indicates that higher torsional strain amplitudes primarily weaken the material in the shear direction without significantly affecting axial properties. When the frequency increases from $0.5\,\mathrm{Hz}$ to $1\,\mathrm{Hz}$ for either torsional strain amplitude ($\pm 0.1\,\%$ or $\pm 0.2\,\%$), the yield surface changes remain consistent, emphasizing that the cyclic torsion strain amplitude has a more pronounced impact on the yield surface evolution than the frequency. Regardless of the pre-deformation conditions, the compressive yield stress values exhibit minimal variation compared to the initial state, thus indicating that the compressive response is less sensitive to the combined tension-cyclic torsion pre-deformation.

These findings highlight the complex interplay of the strain amplitude, the frequency, and the stress direction in determining the anisotropic evolution of the yield surface. The behaviour of CP-Cu under combined preloading reflects its unique response, which may be influenced by factors such as dislocation interactions, texture development, and a strain path. Although similar studies have explored the yield surface evolution in different materials, variations in material properties, microstructures, and loading conditions make direct comparisons challenging. This highlights the importance of tailored investigations for specific materials and preloading scenarios to fully understand their mechanical responses.

The coefficients of the Szczepiński yield equation were calculated using the least squares method to fit the experimental data and describe the elliptical yield surface of the tested material.

This approach minimizes the sum of squares of the distances between the experimental yield points and the approximation curve, ensuring an optimal representation of the yield surface. Table 3 summarizes the fitting errors for each yield surface determined during the analysis. The fitting error values were minimal across all cases, demonstrating a high degree of accuracy in matching the experimental data with the fitted ellipses. These low errors validate the reliability and precision of the Szczepiński anisotropic yield criterion in approximating the yield behaviour of the material. The accuracy of the fitting not only confirms the robustness of the Szczepiński model but also highlights its ability to account for the material's anisotropy effectively. By closely representing the experimental data, the model captures the features of the yield surface evolution, such as the influence of pre-deformation, stress directionality, and anisotropic hardening or softening effects. This agreement further highlights the suitability of the Szczepiński criterion for characterizing the complex mechanical behaviour of the tested material under multiaxial stress states, providing a reliable foundation for predictive modelling and material design.

Table 3. Yield surfaces fitting errors for CP-Cu in as-received state and after pre-deformation.

As-received	Monotonic tension deformed	±0.1 % at 0.5 Hz deformed	±0.2 % at 0.5 Hz deformed	±0.1 % at 1 Hz deformed	±0.2 % at 1 Hz deformed
1.95E-01	1.01E-01	1.58E-01	7.18E-02	1.63E-01	8.77E-02

Figure 8 highlights the evolution of the elliptical parameters representing the yield surface (*YS*) of CP-Cu in the pre-deformed state compared to the as-received state. Pre-deformation through monotonic tension, represented by 0 % cyclic torsion strain amplitude, shows minimal deviations in the axis ratio relative to the yield surface of the material in the as-received state (1.34). However, the combined tension-cyclic torsion pre-deformation significantly alters
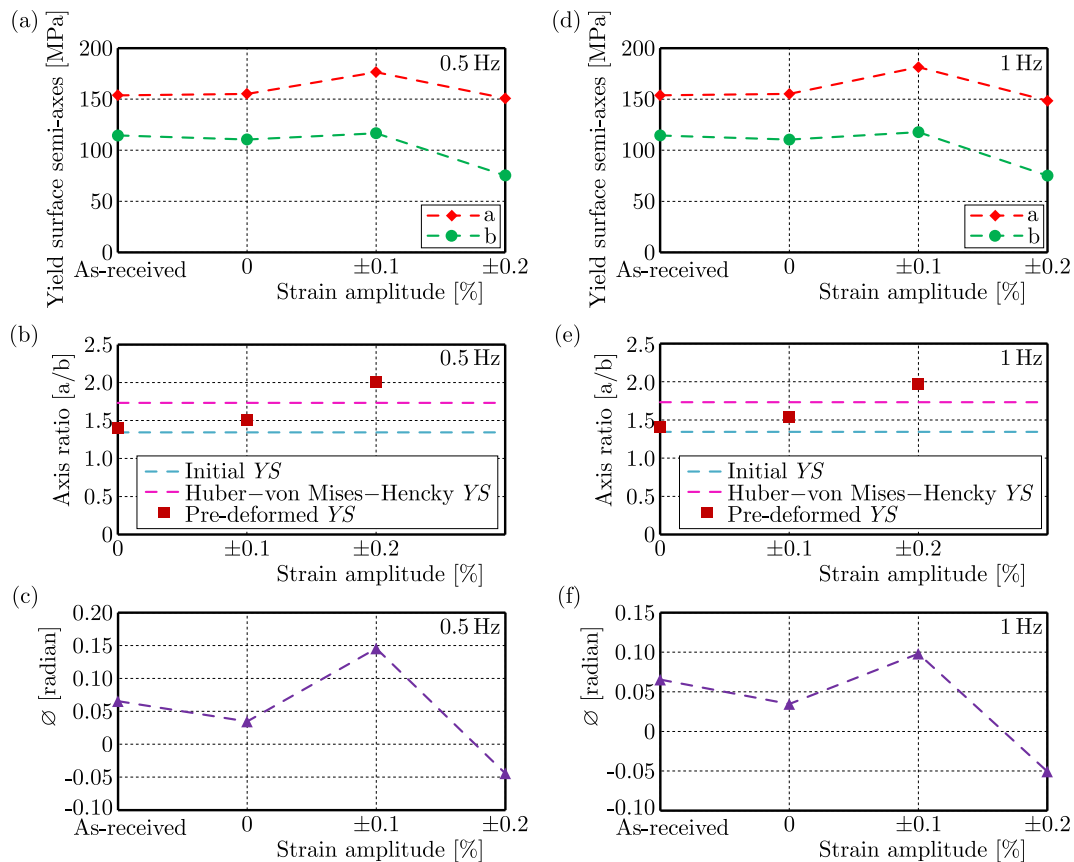

Fig. 8. CP-Cu yield surface parameters evolution caused by tension and combined tension-cyclic torsion pre-deformation (±0.1 % and ±0.2 % strain amplitudes, 0.5 Hz and 1 Hz frequencies).

the axis ratio, with higher values observed at both 0.5 Hz and 1 Hz cyclic torsion frequencies (Figs. 8b and 8e). The highest axis ratio, reaching 2, occurs after pre-deformation with a cyclic torsion strain amplitude of $\pm 0.2\%$ at 0.5 Hz, indicating substantial anisotropic behaviour.

The rotation angle ($\varnothing$) of the YS-axes with respect to the (σ_{xx}, τ_{xy}) coordinate system further reflects the influence of pre-deformation. As shown in Figs. 8c and 8f, monotonic tension pre-deformation results in near-zero rotation, signifying minimal distortion in the YS orientation. In contrast, the combined tension-cyclic torsion pre-deformation induces distinct rotations: positive angles (counter-clockwise) for a cyclic torsion strain amplitude of $\pm 0.1\%$ and negative angles (clockwise) as the strain amplitude increases to $\pm 0.2\%$ at both 0.5 Hz and 1 Hz frequencies. These rotations highlight the directional sensitivity of anisotropic behaviour induced by cyclic torsion and its dependence on strain amplitude.

Figure 9 presents a further analysis of the YS centre positions, emphasizing the role of back stress components in pre-deformed materials. In the as-received state, the YS centre aligns closely with the origin, reflecting minimal back stress. However, pre-deformation through monotonic tension and combined tension-cyclic torsion at $\pm 0.1\%$ strain amplitude shows a significant shift in the YS centre, indicating elevated back stress. In contrast, the combined tension-cyclic torsion at higher strain amplitudes ($\pm 0.2\%$) results in minimal back stress, suggesting a redistribution of internal stresses. The observed back stress arises from dislocation interactions, including the accumulation of geometrically necessary dislocations (GNDs) and their ability to impede further dislocation motion. These interactions create localized high-stress regions that influence the material's plastic behaviour. The findings emphasize the interplay between dislocation structures, strain amplitude, and the stress state in shaping the yield surface evolution of CP-Cu.
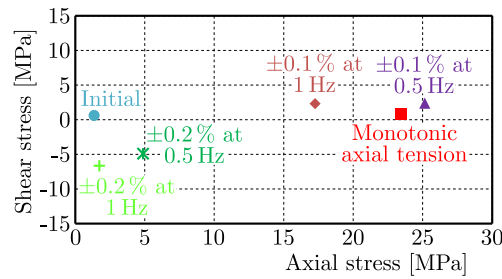

Fig. 9. Centre of yield surfaces of CP-Cu in as-received and pre-deformed states.

Figure 10 presents a comprehensive visualization of the evolution of the initial yield surface in the axial-shear stress space, derived from experimental data following material pre-deformation at frequencies of 0.5 Hz and 1 Hz. The results reveal distinct yield surface shapes and significant variations in their dimensions depending on the pre-deformation loading conditions. For monotonic tension combined with cyclic torsion at a strain amplitude of $\pm 0.1\%$, the yield surfaces at both frequencies exhibit the largest dimensions among all loading conditions. This indicates that even at a low strain amplitude, cyclic torsion induces pronounced hardening effects in the material.
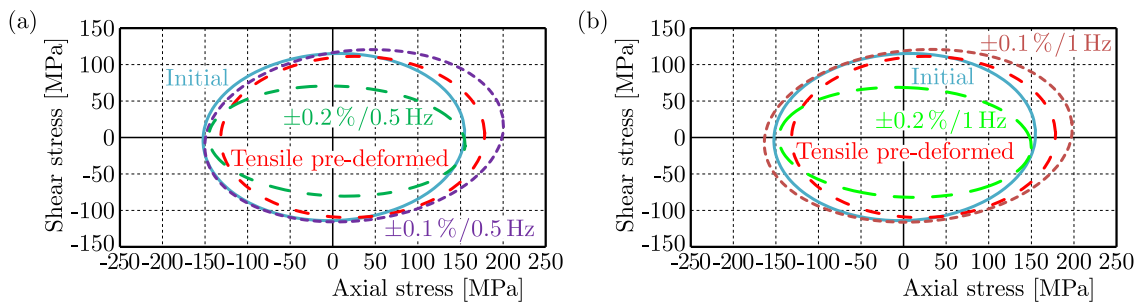

Fig. 10. Comparison of CP-Cu yield surfaces in as-received state and after pre-deformation.

A detailed examination of the yield surfaces highlights two primary hardening mechanisms: kinematic and isotropic. After the monotonic tension pre-deformation, the yield surface shifts in the direction of axial pre-deformation. This translation indicates kinematic hardening, which reflects the material's increased resistance to plastic flow in the pre-deformation direction, likely due to the accumulation of dislocations and directional stress-induced anisotropy. On the other hand, when cyclic torsion ($\pm 0.1\%$ strain amplitude) is introduced during monotonic tensile pre-deformation, nearly isotropic hardening is observed in comparison to the monotonic tensile pre-deformed yield surface. This is demonstrated by the expansion of the yield loci compared to those resulting from monotonic tension alone. The presence of a small cyclic torsion facilitates a more distributed microstructural rearrangement, leading to an overall increase in the material strength across all stress directions. This effect is consistent across both frequencies ($0.5\,\mathrm{Hz}$ and $1\,\mathrm{Hz}$), emphasizing that the strain amplitude, rather than the frequency, is the dominant factor influencing isotropic hardening.

Furthermore, the analysis of yield surface shapes highlights a clear dependency on the preloading direction. The directional nature of pre-deformation, whether purely axial or combined with torsional components, governs the stress distribution and subsequent yield surface dimensions. The axial preloading emphasizes anisotropic hardening effects, while the addition of small torsional components promotes more uniform strengthening across stress states. However, a larger torsional component during axial preloading led to anisotropic softening. These findings emphasize the complex relationships between preloading conditions, the strain path, and the resulting hardening/softening mechanisms. Understanding these effects is essential for modelling the mechanical behaviour of CP-Cu accurately and optimizing its performance in applications involving multiaxial loading and pre-deformed states. While the explanation of hardening or softening behaviour of the yield surface of CP-Cu is supported by deformation theories and previous research, microstructural investigations will be essential for further validation in subsequent studies.

4. Concluding remarks

The comprehensive investigation into the yield surface evolution of commercially pure copper under monotonic tension and combined tension-cyclic torsion loading has provided insights into its mechanical response and hardening/softening behaviour. The key findings are summarized as follows:

– Pre-deformation, whether through monotonic tension or combined tension-cyclic torsion, significantly changes the shape, size, and position of the yield surface. Monotonic tension induces kinematic hardening, translating the yield surface in the pre-strain direction, while combined tension-cyclic torsion ($\pm 0.1\%$ strain amplitude) introduces anisotropic hardening, in comparison to the initial yield loci. Higher torsional strain amplitude during pre-deformation ($\pm 0.2\%$) leads to anisotropic softening, especially in the shear stress direction, reflecting the complex interplay between the loading direction and the strain path.

– The cyclic torsion strain amplitude significantly impacts the material's mechanical response, with higher amplitudes ($\pm 0.2\%$) causing pronounced softening effects, maybe due to increased dislocation interactions and microstructural rearrangements. Conversely, the cyclic torsion frequency has a comparatively lesser impact, with the yield surface evolution remaining consistent across frequencies ($0.5\,\mathrm{Hz}$ and $1\,\mathrm{Hz}$). This underscores strain amplitude as the dominant factor influencing the hardening or softening mechanisms in CP-Cu.

– The initial yield surface of the as-received copper at 0.01% and 0.005% offset strain demonstrates anisotropic behaviour, as indicated by deviations from the isotropic Huber–von Mises–Hencky (HMH) criterion. Additionally, the yield surface is influenced by the

specific definition of the yield used. This anisotropy is likely a result of the material's manufacturing process or specimen machining, which can introduce crystallographic textures, residual stresses, and microstructural inconsistencies. Further evidence of elastic anisotropy is seen in the variations of Young's modulus across different loading directions, highlighting the need to account for these factors when modelling the material's behaviour.

– The Szczepiński anisotropic yield criterion, fitted using the least squares method, effectively captured the experimental yield surfaces with minimal fitting errors. This model accurately represents anisotropic and isotropic hardening behaviours, providing a robust framework for predicting the mechanical response of CP-Cu under multiaxial stress states.

Acknowledgments

References

1. Czerwinski, F. (2024). Aluminum alloys for electrical engineering: a review. *Journal of Materials Science*, *59*(32), 14847–14892. https://doi.org/10.1007/s10853-024-09890-0

2. Davis, J.R. (2001). *Copper and copper alloys*. In J.R. Davis (Ed.), Alloying: Understanding the basics (pp. 457–494). ASM International. https://doi.org/10.31399/asm.tb.aub.t61170457

3. Dietrich, L., & Kowalewski, Z.L. (1997). Experimental investigation of an anisotropy in copper subjected to predeformation due to constant and monotonic loadings. *International Journal of Plasticity*, *13*(1–2), 87–109. https://doi.org/10.1016/S0749-6419(97)00002-8

4. Dubey, V.P., Kopec, M., Łazińska, M., & Kowalewski, Z.L. (2023). Yield surface identification of CP-Ti and its evolution reflecting pre-deformation under complex loading. *International Journal of Plasticity*, *167*, Article 103677. https://doi.org/10.1016/j.ijplas.2023.103677

5. Gazder, A.A., Dalla Torre, F., Gu, C.F., Davies, C.H.J., & Pereloma, E.V. (2006). Microstructure and texture evolution of bcc and fcc metals subjected to equal channel angular extrusion. *Materials Science and Engineering: A*, *415*(1–2), 126–139. https://doi.org/10.1016/j.msea.2005.09.065

6. Guschlbauer, R., Momeni, S., Osmanlic, F., & Körner, C. (2018). Process development of 99.95% pure copper processed via selective electron beam melting and its mechanical and physical properties. *Materials Characterization*, *143*, 163–170. https://doi.org/10.1016/j.matchar.2018.04.009

7. Hecker, S.S. (1971). Yield surfaces in prestrained aluminum and copper. *Metallurgical Transactions*, *2*(8), 2077–2086. https://doi.org/10.1007/BF02917534

8. Helling, D.E., Miller, A.K., & Stout, M.G. (1986). An experimental investigation of the yield loci of 1100-0 aluminum, 70:30 brass, and an overaged 2024 aluminum alloy after various prestrains. *Journal of Engineering Materials and Technology*, *108*(4), 313–320. https://doi.org/10.1115/1.3225888

9. Jadhav, S.D., Goossens, L.R., Kinds, Y., Van Hooreweder, B., & Vanmeensel, K. (2021). Laser-based powder bed fusion additive manufacturing of pure copper. *Additive Manufacturing*, *42*, Article 101990. https://doi.org/10.1016/j.addma.2021.101990

10. Jiang, Q., Zhang, P., Yu, Z., Shi, H., Wu, D., Yan, H., Ye, X., Lu, Q., & Tian, Y. (2021). A review on additive manufacturing of pure copper. *Coatings*, *11*(6), Article 740. https://doi.org/10.3390/coatings11060740

11. Kopec, M., Dubey, V.P., Pawlik, M., Wood, P., & Kowalewski, Z.L. (2024). Experimental identification of yield surface for additively manufactured stainless steel 316L under tension–compression-torsion conditions considering its printing orientation. *Manufacturing Letters*, *41*, 28–32. https://doi.org/10.1016/j.mfglet.2024.07.003

12. Lai, Z., Mai, Y., Song, H., Mai, J., & Jie, X. (2022). Heterogeneous microstructure enables a synergy of strength, ductility and electrical conductivity in copper alloys. *Journal of Alloys and Compounds*, *902*, Article 163646. https://doi.org/10.1016/j.jallcom.2022.163646

13. Li, M., & Zinkle, S.J. (2012). 4.20 – Physical and mechanical properties of copper and copper alloys. *Comprehensive Nuclear Materials*, *4*, 667–690. https://doi.org/10.1016/B978-0-08-056033-5.00122-1

14. Liu, C., Yang, X., Ding, Y., Li, H., Wan, S., Guo, Y., & Li, Y. (2023). The yielding behavior of TU00 pure copper under impact loading. *International Journal of Mechanical Sciences*, *245*, Article 108110. https://doi.org/10.1016/j.ijmecsci.2023.108110

15. Mair, W.M., & Pugh, H.Ll.D. (1964). Effect of pre-strain on yield surfaces in copper. *Journal of Mechanical Engineering Science*, *6*(2), 150–163. https://doi.org/10.1243/JMES_JOUR_1964_006_025_02

16. Pan, Q., Jing, L., & Lu, L. (2023). Enhanced fatigue endurance limit of Cu through low-angle dislocation boundary. *Acta Materialia*, *244*, Article 118542. https://doi.org/10.1016/j.actamat.2022.118542

17. Pingale, A.D., Owhal, A., Katarkar, A.S., Belgamwar, S.U., & Rathore, J.S. (2021). Recent researches on Cu-Ni alloy matrix composites through electrodeposition and powder metallurgy methods: A review. *Materials Today: Proceedings, 3rd International Conference on Advances in Mechanical Engineering and Nanotechnology*, *47*(Part 11), 3301–3308. https://doi.org/10.1016/j.matpr.2021.07.145

18. Scudino, S., Unterdörfer, C., Prashanth, K.G., Attar, H., Ellendt, N., Uhlenwinkel, V., & Eckert, J. (2015). Additive manufacturing of Cu–10Sn bronze. *Materials Letters*, *156*, 202–204. https://doi.org/10.1016/j.matlet.2015.05.076

19. Semih, Ö., & Recep, A. (2023). Investigation of microstructure, machinability, and mechanical properties of new-generation hybrid lead-free brass alloys. *High Temperature Materials and Processes*, *42*(1), Article 20220263. https://doi.org/10.1515/htmp-2022-0263

20. Stepanov, N.D., Kuznetsov, A.V., Salishchev, G.A., Raab, G.I., & Valiev, R.Z. (2012). Effect of cold rolling on microstructure and mechanical properties of copper subjected to ECAP with various numbers of passes. *Materials Science and Engineering: A*, *554*, 105–115. https://doi.org/10.1016/j.msea.2012.06.022

21. Sundar Singh Sivam, S.P., Rajendran, R., & Harshavardhana, N. (2023). An investigation of stored energy in uniaxial and biaxial directional rolling on mechanical properties and microstructure of pure copper. *Mechanics Based Design of Structures and Machines*, *51*(5), 2831–2843. https://doi.org/10.1080/15397734.2021.1909484

22. Vahedi Nemani, A., Ghaffari, M., Sabet Bokati, K., Valizade, N., Afshari, E., & Nasiri, A. (2024). Advancements in additive manufacturing for copper-based alloys and composites: A comprehensive review. *Journal of Manufacturing and Materials Processing*, *8*(2), Article 54. https://doi.org/10.3390/jmmp8020054

23. Wu, X.X., San, X.Y., Gong, Y.L., Chen, L.P., Li, C.J., & Zhu, X.K. (2013). Studies on strength and ductility of Cu–Zn alloys by stress relaxation. *Materials & Design*, *47*, 295–299. https://doi.org/10.1016/j.matdes.2012.12.020

24. Zhang, W.-J., Huang, L., Mi, X.-J., Xie, H.-F., Feng, X., & Ahn, J.H. (2024). Researches for higher electrical conductivity copper-based materials. *cMat*, *1*(1), e13. https://doi.org/10.1002/cmt2.13

25. Zhou, M., Geng, Y., Zhang, Y., Ban, Y., Li, X., Jia, Y., Liang, S., Tian, B., Liu, Y., & Volinsky, A.A. (2023). Enhanced mechanical properties and high electrical conductivity of copper alloy via dual-nanoprecipitation. *Materials Characterization*, *195*, Article 112494. https://doi.org/10.1016/j.matchar.2022.112494